

## Study of Polymer Layer Characteristics on Al and Ti Alloys

O.V. Tushavina<sup>1</sup>, V.V. Rodchenko<sup>2</sup>, Yan Naing Min

<sup>1</sup>Moscow Aviation Institute (National Research University), Volokolamskoe shosse, 4, 125993, Moscow, Russia

<sup>2</sup>Moscow Aviation Institute (National Research University), Volokolamskoe shosse, 4, 125993, Moscow, Russia

<sup>3</sup>Defence Services Academy (D.S.A), Department of Mathematics Mandalay-Lashio highway street, Pyin Oo Lwin, Mandalay Division, Myanmar.

<sup>3</sup>solgtu@gmail.com

**Article History** Received: 10 January 2021; Revised: 12 February 2021; Accepted: 27 March 2021; Published online: 28 April 2021

**Abstract:** In this work, the mechanical properties of organic coatings based on epoxy resin (DGEBA DER 332) and two diamines comonomers (IPD and 3DCM) were investigated. The coatings were applied to substrates made of aluminum and titanium alloys. Differential scanning calorimetry and infrared spectroscopy were used to study the effect of the coating thickness on the degree of reaction of the substrate of both alloys and compare with the volumetric values. The residual stress and Young's modulus of the coatings were calculated using one-dimensional analysis based on beam theory with the introduction of a biaxial modulus for isotropic stress (thin plate theory). A stiffness factor was introduced, since deformations in the coating lead to deformations in the substrate. During the thermal cure cycle, a loss of curing agent was observed and thus a change in the degree of reaction of the coating.

**Keywords:** Polymer coatings, substrates, Young's modulus, residual stresses.

### 1. Introduction

Modulus of elasticity and residual stresses are among the most important mechanical properties of coating materials and their importance plays an important role in applied and/or fundamental fields. Two-layer materials (coatings of different thicknesses are applied to a metal substrate) are used in many industries (aerospace, automotive, electronics, etc.) [1-5]. Understanding and modeling the mechanical behavior (practical adhesion, wear, friction, protective properties) requires knowledge of the Young's modulus of both the substrate and the coating, as well as the determination of the residual stresses created at the interface between the polymer and the substrate and/or in the organic layer [6-15]. For example, high levels of residual stresses are undesirable as they can lead to deformations, cracks or poor adhesion of the coating. Many studies have been carried out to determine the residual stresses within the coating [16-25]. Most of them concern stresses in thin coatings (the coating thickness is less than the substrate thickness), in which the authors widely use and improve the one-dimensional Stoney method using the theory of beams. In recent publications, various expressions have been obtained for the first order residual stresses within a coating applied to sheet substrates, taking into account in-plane deformations in two-layer systems, by introducing biaxial models for isotropic stresses (theory of thin plates) [26-31]. When deformation of the coating causes deformation of the substrate (with deformation in the plane of the two-layer system), the equation for the residual stress was expressed as a function of the stiffness ratio, which leads to:

$$\left(\sigma_x^0\right)_c = -\frac{E_s h_s^2}{6 h_c (1 - \nu_s) R} \times \frac{1}{(1 + \alpha^* \beta)}$$

$$\times \left[ 1 + \beta (4\alpha^* - 1) + \beta^2 \left[ \alpha^{*2} (\beta - 1) + 4\alpha^* + \frac{(1 - \alpha^*)^2}{1 + \beta} \right] \right]$$

with

$$\alpha^* = \frac{E_c (1 - \nu_s)}{E_s (1 - \nu_c)}$$

and

$$\beta = h_c / h_s$$

where  $h_c$  – coating thickness,  $h_s$  – pad thickness,  $E_c$  – Young's modulus of coverage,  $E_s$  – Young's modulus of the substrate,  $\nu_c$  – Poisson's ratio of coverage,  $\nu_s$  – substrate Poisson's ratio,  $R$  – radius of curvature of the coated system.

It is assumed that the materials forming the two-layer systems are homogeneous, isotropic and elastic. It is also assumed that the distribution of residual stresses within the coating is constant throughout the coating thickness. For thick covers, it is necessary to invert the subscripts  $c$  and  $s$  to the ratios shown above.

Models for curved beams were used to determine Young's modulus of coating materials experiencing residual stresses. Bending stiffness  $(EI)_{eq}^*$  was expressed as a function (a) of the original radius of curvature  $R_1$ , generated by residual stresses developing in the coatings, (b) mechanical radius of curvature  $R_2$  when testing for bending, and (c) mechanical (Young's modulus) and geometric (width and thickness) characteristics of two-layer systems. Young's modulus of a two-layer system is calculated from the slope of the load curve within the linear deformation region (obtained from the bending test), while the ratio of span to sample thickness is infinite. Young's modulus of the coating with residual stresses was calculated using the following relation:

$$E_c^{*3} (I_c h_c^2) + E_c^{*2} \left[ I_c h_c h_s E_s \left( 2 - \frac{R_2}{R_1} \right) + h_c^2 (E_s h_s H - X^*) \right] \\ + E_c^* \left[ -X^* E_s h_s (h_c + h_s) + S_c E_s^2 h_s^2 (2h_c^2 + 3h_c h_s + 2h_s^2) \frac{R_2}{6R_1} \right. \\ \left. + h_s^2 (I_c + S_c H) \right] - E_s^2 h_s^2 \left( E_s I_s \frac{R_2}{R_1} + X^* \right) \\ = 0$$

with

$$X^* = (EI)_{eq}^* (1 - R_2/R_1) - E_s I_s$$

$$H = \left( \frac{h_c}{2} + \frac{h_s}{2} \right)^2$$

$$S_c = b_c h_c$$

$$I_c = b_c h_c^3 / 12$$

and

$$I_s = b_s h_s^3 / 12$$

where  $b_c$  – cover width,  $b_s$  – substrate width,  $E_{c^*}$  - Young's modulus of the cover with stresses. Only positive roots were considered.

This study focuses on determining the elastic moduli and residual stresses of coating materials depending on substrate material (with and without surface treatment), polymer, curing conditions and coating thickness. Typically, surface treatment of substrates is used to improve the practical adhesion of coatings. During processing, the surface acidity of the substrate changes and the nature of the interaction of the components of the coating and the substrate changes. The composition and formation of the coating network near the substrate surface can be quite different compared to the bulk coating with the formation of a “coating/substrate” interfacial layer. Consequently, during curing, the phenomenon of concentrated residual stresses in the coatings and the viscoelastic properties (Young's modulus) of the coating may also change. Finally, as the curing temperature rises, some of the coating components may partially evaporate (for example, loss of the hardener during the curing of thermosetting material).

## 2. Study of the properties of polymer coatings

We used metal substrates from an aluminum alloy (2024) and a titanium alloy (Ti6Al4V) with a thickness of 511  $\mu\text{m}$  and 426  $\mu\text{m}$ , respectively. Poisson's ratios are taken from the handbook and are equal to 0,3 for both substrates. Before using any of the polymers, the surface of the aluminum and titanium substrate was treated by ultrasonic degreasing with acetone for 10 min. and in ethyl acetate for 10 minutes (Table 1).

Table 1. Surface treatment of aluminum and titanium alloys.

Alloy	Treatment	Description
Aluminum	Degreasing	Ultrasonic degreasing with acetone for 10 min. and in ethyl acetate for 10 minutes.
	Chemical etching	Immersion in a solution of 250 g of sulfuric acid, 50 g of chromic acid and distilled water up to 1 liter.
Titanium	Degreasing	Ultrasonic degreasing with acetone for 10 min. and in ethyl acetate for 10 minutes.
	Chemical etching	Immersion in an ammonium bifluoride solution (10 g / L) at room temperature for 2 minutes.

After processing, all substrates were kept indoors at room temperature. No changes in the substrate thickness after chemical etching were found.

For analysis, titanium and aluminum sheets were cut into 100 mm by 100 mm squares. After surface treatment, coatings of various thicknesses (100, 200, 300, and 500 μm) were applied. Several layers of adhesive tape were applied around the periphery of the processed sheet to obtain the desired wet film thickness. The epoxy resin was poured onto a metal surface and smeared with a cylindrical glass rod. The polymer was applied no more than two hours after the substrate surface was treated. For mechanical tests (to determine Young's modulus and residual stress of organic coatings), coated samples were prepared using a silicone mold (shown in Fig. 1).

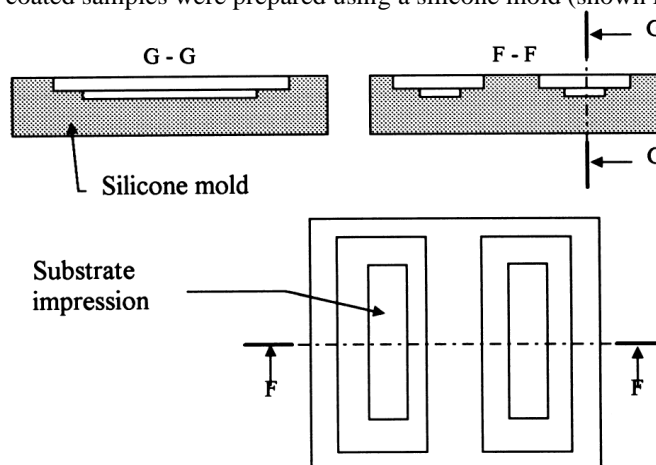


Fig. 1. Sample testing scheme.

After curing and cooling, the thickness of the adhesive coatings was determined using a micrometer (sensitivity 5 μm).

Used commercial monomers are shown in Table 2. All chemicals were used without further purification. The stoichiometric ratio R (amine hydrogen / epoxy resin) is 1.

Table 2  
Chemical structure of various monomers<sup>a</sup>

Notation	Formulae	Supplier
DGEBA (1)		Dow Chem. DER 332
3DCM (2)		Hüls C260
IPD (3)		Veba Chemie

The homogeneity of the mixture of DGEBA and hardener (3DCM or IPD) was achieved by stirring under primary vacuum at 408 C° (rotary evaporator RE 211, Switzerland) for 1 hour to avoid the ingress of gas bubbles. Then the corresponding volumes of the mixture were applied to metal substrates or in the cavity of the mold no later than 2 hours after the treatment of the substrate. Curing conditions are given for each dataset.

For thermal analysis, bulk polymers were prepared using a cavity (70mm/10mm/20mm) in a PTFE mold. After curing and cooling, the specimens were cut to the desired thickness using a mechanical diamond saw.

To determine Young's modulus, rods were made from epoxy polymers (the same epoxy was used for bars and coatings) using a silicone mold (4.5 mm / 5 mm / 80 mm). Poisson's ratios for epoxy-amine polymers are 0,3.

The glass transition temperature ( $T_g$ ) was determined using a differential scanning calorimeter at a rate of 10 C°/min from 0 to 250 C°. A 40 µL aluminum crucible with a pin hole was used. The calorimeter was calibrated with cyclohexane and indium. Samples were weighed on a balance (Mettler Toledo) with a sensitivity of 1 µg.

An infrared spectrometer (FTIR Magna-IR 550 from Nicolet) with Omnic FTIR software was used. EverGloe source was used together with KBr beam splitter and DTGS-KBr detector. In the mid-infrared region, spectra were recorded in the range from 400-4000  $cm^{-1}$  and in the range 4000-7000  $cm^{-1}$  for the near infrared region of the spectrum. Assisted transmission has been used for bulk or free constant film characteristics. KBr was mixed in a ratio of 1:100 with various epoxy powders. Thin epoxy powder coatings were obtained by combing with a blade. The cKBr mixture was vacuum pressed to form discs. Blank discs were used as background. For using the spectrometer in the range of angles from 30 to 80 degrees, used a variable angle specular instrument for the samples to be analyzed. In this case, treated metal substrates were used as a background. For each analysis, 32 and 64 scans were collected at a resolution 4  $cm^{-1}$ .

Experiments to measure the radius of curvature were carried out on a loading device equipped with a full-scale load cell with a sensitivity of 5 mN and a range of 20 N. A two-layer bar was placed on a flat and rigid material. The curvature was measured after the deposition and curing of the coating layer on the substrate. The cover and backing are of the same width. The curved shape of the multilayer strip is characterized by a circular arc (i.e., there is a single radius of curvature). The maximum deflection ( $\delta_{max}$ ) of the convex bottom side is determined for each coated system. If we assume that the radius of curvature is large in comparison with the length and width of the two-layer bar, then we can assume that the length of the neutral axis is equal to its span. Thus, for such a curved two-layer bar with a neutral line equal to L, the maximum deviation  $\delta_{max}$  in the average swing L/2 the radius of curvature  $R_1$  is:

$$R_1 = L^2/8\delta_{max}$$

Glass transition temperature and change in specific heat were measured using DSC. The characteristics  $T_{g0}$  and  $\Delta C_{p0}$  of the initial epoxy-amine mixture were determined from the first thermogram. The characteristics  $T_{g1}$  and  $\Delta C_{p1}$  of the final mixtures were measured from the second (or third) thermogram when the heat of exothermic polymerization is zero. The corresponding values are shown in Table 3. The data coincided with the theoretical.

Table 3  
Glass transition temperature and specific heat capacity values for the initial state and the final network of the two epoxy systems (DGEBA/IPD and DGEBA/3DCM)

System	$\Delta C_{p0}$ (J/g K)	$\Delta C_{p\infty}$ (J/g K)	$T_{g0}$ (°C)	$T_{g\infty}$ (°C)
DGEBA-3DCM	0.59	0.19	- 32	183
DGEBA-IPD	0.56	0.24	- 45	157

The degree of polymerization (x) can be calculated as follows:

$$\frac{T_g - T_{g0}}{T_{g\infty} - T_{g0}} = \frac{\lambda x}{1 - (1 - \lambda x)}$$

where  $T_g$  – glass transition temperature at any degree of polymerization and  $\lambda$  – adjustable parameter. Wherein:

$$\lambda = \Delta C_{p\infty}/\Delta C_{p0}$$

For the DGEBA/IPD and DGEBA/3DCM epoxy-amine systems, the  $\lambda$  values were 0,42 and 0,32 respectively. Then, from the  $T_g$ , values obtained for the various coatings and bulk materials, x can be calculated depending on the nature of the substrate and its processing, film thickness and cure cycle.

It was noted that under the same curing conditions, the  $T_g$  values for bulk epoxy-amine systems were always higher than those obtained for the coated materials. In addition,  $T_g$  increases with increasing coating thickness. DSC failed to observe any significant effect associated with the nature of the substrate.

### 3. Conclusion

The glass transition temperature, polymerization temperature, nature and intensity of residual stresses, Young's modulus of DGEBA organic coatings based on epoxy resin and two diamine curing agents (IPD and 3DCM) were measured in comparison with the volumetric values. The coatings were applied to aluminum and titanium substrates. It was found that all these properties depend on the nature of the substrate and its surface treatment, on the nature of the hardener and curing conditions, and on the thickness of the coating. Curing was observed with loss of agent during the thermal cure cycle.

### 4. Acknowledgements

The work was carried out with the financial support of the state project of the Ministry Science and Higher Education of the Russian Federation "Theoretical and experimental research in production and processing of advanced metal and composite materials based on aluminum and titanium alloys", project No. FSFF-2020-0016.

### References

1. Kuznetsova, E.L., Rabinskiy, L.N. Heat transfer in nonlinear anisotropic growing bodies based on analytical solution // *Asia Life Sciences*, 2019, (2), p. 837–846.
2. Kuznetsova, E.L., Rabinskiy, L.N. Numerical modeling and software for determining the static and linkage parameters of growing bodies in the process of non-stationary additive heat and mass transfer//*Periodico Tche Quimica*, 2019, 16(33), p. 472–479.
3. Kuznetsova, E.L., Rabinskiy, L.N. Linearization of radiant heat fluxes in the mathematical modeling of growing bodies by the action of high temperatures in additive manufacturing // *Asia Life Sciences*, 2019, (2), p. 943–954.
4. Rabinsky, L.N., Kuznetsova, E.L. Simulation of residual thermal stresses in high-porous fibrous silicon nitride ceramics // *Powder Metallurgy and Metal Ceramics*, 2019, 57(11-12), p. 663–669.
5. Rabinskiy, L.N. Non-stationary problem of the plane oblique pressure wave diffraction on thin shell in the shape of parabolic cylinder// *Periodico Tche Quimica*, 2019, 16(32), p. 328–337.
6. Formalev, V.F., Kolesnik, S.A., Kuznetsova, E.L. Analytical study on heat transfer in anisotropic space with thermal conductivity tensor components depending on temperature//*Periodico Tche Quimica*, 2018, 15(Special Issue 1), p. 426–432.
7. Formalev, V.F., Kolesnik, S.A. Temperature-dependent anisotropic bodies thermal conductivity tensor components identification method// *International Journal of Heat and Mass Transfer*, 2018, 123, p. 994–998.
8. Formalev, V.F., Kolesnik, S.A., Kuznetsova, E.L. Analytical solution-based study of the nonstationary thermal state of anisotropic composite materials // *Composites: Mechanics, Computations, Applications*. 2018. 9(3), p. 223-237.
9. Formalev, V.F., Kolesnik, S.A. On Thermal Solitons during Wave Heat Transfer in Restricted Areas // *High Temperature*, 2019, 57(4), p. 498–502.
10. Formalev, V.F., Kolesnik, S.A., Kuznetsova, E.L., Rabinskiy, L.N. Origination and propagation of temperature solitons with wave heat transfer in the bounded area during additive technological processes // *Periodico Tche Quimica*. 2019. 16(33), p. 505-515.
11. Formalev, V.F., Kolesnik, S.A., Kuznetsova, E.L. Mathematical modeling of a new method of thermal protection based on the injection of special coolants // *Periodico Tche Quimica*. 2019.16(32), p. 598-607.
12. Formalev, V.F., Kolesnik, S.A. On Inverse Coefficient Heat-Conduction Problems on Reconstruction of Nonlinear Components of the Thermal-Conductivity Tensor of Anisotropic Bodies // *Journal of Engineering Physics and Thermophysics*. 2017. 90(6), p. 1302-1309.
13. Formalev, V.F., Kolesnik, S.A. Analytical investigation of heat transfer in an anisotropic band with heat fluxes assigned at the boundaries // *Journal of Engineering Physics and Thermophysics*. 2016. 89(4), p. 975-984.
14. Formalev, V.F., Kartashov, É.M., Kolesnik, S.A. Simulation of Nonequilibrium Heat Transfer in an Anisotropic Semispace Under the Action of a Point Heat Source// *Journal of Engineering Physics and Thermophysics*. 2019. 92(6), p. 1537-1547.

15. I.S. Kurchatov, N.A. Bulychev, S.A. Kolesnik. Obtaining Spectral Characteristics of Semiconductors of AIIBVI Type Alloyed with Iron Ions Using Direct Matrix Analysis, *International Journal of Recent Technology and Engineering*, 2019, Vol. 8, I. 3, p. 8328-8330.
16. M.O. Kaptakov. Enhancement of Quality of Oil Products under Ultrasonic Treatment, *International Journal of Pharmaceutical Research*, 2020, Vol. 12, Supplementary Issue 2, pp. 1851-1855.
17. Formalev, V.F., Kolesnik, S.A., Kuznetsova, E.L. Identification of new law for decomposition of bonding heat-shielding composite materials/*Asia Life Sciences*. 2019. (1), p. 139-148.
18. Kuznetsova, E.L., Makarenko, A.V. Mathematical model of energy efficiency of mechatronic modules and power sources for prospective mobile objects // *Periodico Tche Quimica*, 2019, 16 (32), p. 529–541.
19. Rabinskiy, L.N., Kuznetsova, E.L. Analytical and numerical study of heat and mass transfer in composite materials on the basis of the solution of a stefan-type problem// *Periodico Tche Quimica*, 2018, 15 (Special Issue 1), p. 339–347.
20. Bulychev, N.A., Kuznetsova, E.L. Ultrasonic Application of Nanostructured Coatings on Metals// *Russian Engineering Research*, 2019, 39 (9), p. 809–812.
21. M.O. Kaptakov. Catalytic Desulfuration of Oil Products under Ultrasonic Treatment, *International Journal of Pharmaceutical Research*, 2020, Vol. 12, Supplementary Issue 2, pp. 1838-1843.
22. Bulychev, N.A., Bodryshev, V.V., Rabinskiy, L.N. Analysis of geometric characteristics of two-phase polymer-solvent systems during the separation of solutions according to the intensity of the image of micrographs//*Periodico Tche Quimica*, 2019, 16(32), p. 551–559.
23. Bodryshev V. V., Rabinskiy L.N., Nartova L.G., Korzhov N.P. Geometry analysis of supersonic flow around two axially symmetrical bodies using the digital image processing method // *Periódico Tchê Química*. 2019. vol. 16, no. 33, pp. 541-548.
24. Bulychev N. A., Kazaryan M.A., Erokhin A.I., Averyushkin A.S., Rabinskii L.N., Bodryshev V. V., Garibyan B.A. Analysis of the Structure of the Adsorbed Polymer Layers on the Surfaces of Russian Metallurgy (Metally), Vol. 2019, No. 13, pp. 1319–1325.
25. Formalev, V.F., Kolesnik, S.A., Selin, I.A. Local non-equilibrium heat transfer in an anisotropic half-space affected by a non-steady state point heat source // *Herald of the Bauman Moscow State Technical University, Series Natural Sciences*. 2018. 80(5), p. 99-111.
26. Kolesnik, S.A., Bulychev, N.A., Rabinskiy, L.N., Kazaryan, M.A. Mathematical modeling and experimental studies of thermal protection of composite materials under high-intensity effects of laser radiation// *Proceedings of SPIE - The International Society for Optical Engineering*. 2019. 11322, article number 113221R.
27. Kuznetsova, L. E., Fedotenkov, V. G. Dynamics of a spherical enclosure in a liquid during ultrasonic cavitation // *Journal of Applied Engineering Science*. 2020. 18(4), p. 681 - 686.
28. Makarenko, A.V., Kuznetsova, E.L. Energy-Efficient Actuator for the Control System of Promising Vehicles // *Russian Engineering Research*. 2019. 39(9), p. 776-779.
29. Kuznetsova, E.L., Makarenko, A.V. Mathematic simulation of energy-efficient power supply sources for mechatronic modules of promising mobile objects// *Periodico Tche Quimica*, 2018, 15(Special Issue 1), p. 330-338.
30. Li, Y., Arutiunian, A.M., Kuznetsova, E.L., Fedotenkov, G.V. Method for solving plane unsteady contact problems for rigid stamp and elastic half-space with a cavity of arbitrary geometry and location // *INCAS Bulletin*, 2020, 12(Special Issue), p. 99–113.
31. Kuznetsova, E.L., Fedotenkov, G.V., Starovoitov, E.I. Methods of diagnostic of pipe mechanical damage using functional analysis, neural networks and method of finite elements // *INCAS Bulletin*, 2020, 12(Special Issue), p. 79–90.